A Work Project, presented as part of the requirements for the Award of a Master's degree in Economics from the Nova School of Business and Economics.

Mapping socio-economic vulnerability to hydrological risk in Italy. The case of Emilia–Romagna.

Franziska Huber

Work project carried out under the supervision of:

Antonieta Cunha e Sá

20/12/2023

Abstract

This paper investigates the interplay between flood hazard and social vulnerability in Italy's Emilia-Romagna region. It conducts an in-depth, municipal-level analysis to construct a social vulnerability index, highlighting how each socio-economic factor contributes to it. By conducting a correlation analysis and employing Geographic Information Systems (GIS), the study not only maps the spatial variability of social vulnerability but, by integrating these findings with flood hazard maps, it creates a comprehensive social vulnerability exposure map. This research highlights the critical role of social vulnerability assessments in shaping effective flood risk mitigation policies and provides valuable insights for policymakers for their decision-making.

Keywords

Socio-economic vulnerability, Flood hazard, Hydrological Risk, Social vulnerability exposure, GIS, Correlation Analysis, Italy.

This work used infrastructure and resources funded by Fundação para a Ciência e a Tecnologia (UID/ECO/00124/2013, UID/ECO/00124/2019 and Social Sciences DataLab, Project 22209), POR Lisboa (LISBOA-01-0145-FEDER-007722 and Social Sciences DataLab, Project 22209) and POR Norte (Social Sciences DataLab, Project 22209).

1. Introduction

Italy, celebrated for its rich cultural heritage, faces the daunting challenge of increasing natural hazards, including hydrogeological risks such as landslides, floods, and coastal erosion, which pose a significant threat to its population and infrastructure. According to a study carried out by the Institute for Environmental Protection and Research ISPRA, 93.9% of Italian municipalities are at hydrogeological risk, with around 1.3 million individuals at risk of landslides and 6.8 million people at risk of flood, defined as "hydrological risk" (Trigila, et al., 2021). The increased impact of natural hazards, driven by rising population density, inadequate urban planning, and intensified by climate change (Pachauri et al., 2007), is magnified by Italy's unique geological, geomorphological, and climatic factors, rendering it particularly vulnerable to various natural threats. It is essential to recognize that a hazard escalates into a disaster when it impacts an exposed and vulnerable population (Uitto, 1998), a situation that places Italy among the top five European countries in terms of disaster risk and potential economic losses (Welle et al., 2012). Notably, regions like Emilia-Romagna, Tuscany, Campania, Veneto, Lombardy, and Liguria exhibit particularly high vulnerability. Emilia-Romagna, the central focus of this thesis, has experienced a significant impact from flooding, particularly during the hydrological events of 2023. During May of this year, severe weather conditions led to catastrophic flooding, with rivers such as the Montone, Lamone, Senio, and Santerno flooding vast territories. The flooding resulted in 17 fatalities, substantial economic losses amounting to approximately €10 billion, and the displacement of more than 36.000 individuals (Arrighi & Domeneghetti, 2023). These events highlight the acute exposure of the region to hydrological hazards.

Given this background, the research question of this study is to identify the spatial distribution of and analyze the correlation between socio-economic vulnerability and hydrological hazard in Italy through the analysis of the Emilia-Romagna case. It is essential to evaluate social vulnerability to understand how well a society can prepare for, respond to, withstand, and recover from natural disasters (Frigerio et al., 2016). Therefore, the aim is to understand the specific socio-economic characteristics of the population residing in flood-prone areas, such as age, income, unemployment, education or residential property, and examine how social vulnerability can be integrated into flood risk analysis in Italy.

Recognizing that vulnerability to natural disasters results from a combination of geographical exposure and socio-economic conditions, this research contributes to the discourse on disaster risk management by offering an in-depth analysis of how socio-economic factors intersect with natural hazards. It emphasizes the vital role of incorporating socio-economic considerations into territorial planning and emergency response strategies. By combining SVI with flood hazard to create a qualitative social vulnerability exposure (SVE) map, this research aims to provide insights that can enhance the resilience of Emilia-Romagna. While politics and policy play a significant role in allocating resources for risk reduction and prevention efforts, it is essential to acknowledge that complete avoidance of natural events is an unattainable goal.

2. Literature Review

Social vulnerability assessment is a critical tool in understanding how socio-economic factors influence a community's ability to respond to and recover from hazardous events. The theoretical framework established by Alexander (1993) posits that natural hazards escalate to disasters when impacting vulnerable populations. This perspective is crucial in understanding that the severity of a disaster is not only a result of the natural event itself but also of the affected community. Similarly, Adger (2010) emphasizes that vulnerability is not just about exposure to hazards but also about the sensitivity and adaptive capacity of the population. This comprehensive approach is essential for developing effective risk reduction and management strategies. Cutter et al. (2003)

develop this concept further, introducing the notion of differential vulnerabilities. Their work suggests that socio-economic status, race, ethnicity, and gender are key determinants in how communities experience and recover from disasters.

Several frameworks have been developed to assess social vulnerability. Cutter's hazards-of-place vulnerability model (1996) is one of the most significant frameworks, offering a place-based approach to vulnerability analysis. This model has been influential in understanding and quantifying the various socio-economic factors that contribute to a community's overall vulnerability to natural disasters. Building on her earlier work, Cutter, alongside Boruff and Shirley (2003), developed the Social Vulnerability Index (SVI), a tool that quantitatively measures the resilience of communities to environmental hazards. It highlights the multidimensional nature of vulnerability, integrating socio-economic, demographic, and geographic factors. This progression from a general model of vulnerability to a specific, quantifiable index emphasizes the need for tailored, localized approaches in assessing and managing environmental risks. There is however no universally accepted methodology within the scientific community for computing a weighted composite vulnerability index. Consequently, various authors have employed different methods to weight the index. For example, while Cutter et al. (2003) use principal component analysis to systematically create a SVI, Rygel et al. (2006) offer a method that allows for the manual selection and weighting of indicators based on the specific context of the hazard. In the present paper, principal component analysis, as outlined by Cutter et al. (2003), is employed along with the weighting method proposed by Siagian et al. (2014) for the computation of the SVI.

The process of mapping socio-economic vulnerability is crucial for understanding the spatial distribution of risk and resilience. Rufat et al. (2015) discuss various case studies and implications for measuring social vulnerability to floods. Their work provides valuable insights into the methodologies involved in mapping vulnerability at both national and local scales. They also address the methodological challenges, such as data limitations and the necessity of incorporating local specificities, emphasizing the complexity of accurately assessing social vulnerability. According to Rufat et al. (2015), a notable trend in this field is the integration of the hazard-of-place social vulnerability model with exposure metrics like flood damages to quantify risk. Studies in this area include for example Remo et al. (2016), who assess flood vulnerability in Illinois using Hazus-MH, Zhou et al. (2012), who explore economic pluvial flood risk assessment under climate change, and Chen et al. (2019), who use a spatial dependence-based approach for urban flood vulnerability analysis. Other research approaches involve defining flood hazards through statistical flood probability models, as demonstrated by Khajehei et al. (2020), who assess flash flood hazards in the U.S., by Thakuy et al. (2011), who discuss geospatial techniques for environmental management, or by Hoque et al. (2019), who evaluate flood vulnerability in Bangladesh using an analytic hierarchy process. Another category of studies uses satellite imagery for the assessment of flood hazard vulnerability, as in the work of Zheng et al. (2008), who analyze flood vulnerability in China's Huaihe River Basin by examining the relationship between land use, population distribution, and flood hazards.

This study falls within the first category, integrating social vulnerability indicators with flood hazard data. While numerous studies in this area have analyzed the social vulnerability of populations exposed to flood hazards, there remains a scarcity of research that combines the SVI and flood hazard into a unified measure, the Social Vulnerability Exposure (SVE). This metric aims to identify hotspot areas marked by both high flood hazard and high SVI, and areas where these factors diverge. By employing Geographic Information Systems (GIS) and statistical modeling, this research analyzes and maps the spatial variability of SVE in the Italian region of Emilia-Romagna, thereby contributing valuable insights to the field of disaster risk management and resilience planning to flood hazard.

3. Hydrological risk

3.1. Flood Hazard

The Italian Institute for Environmental Protection and Research ISPRA employs a meticulous methodology for evaluating flood hazards and risk. This methodology is in line with the EU Floods Directive (FD) 2007/60/EC and Italian Legislative Decree 49/2010. Article 6 of the European FD mandates that Member States prepare flood hazard and risk maps at the level of hydrographic districts or management units for areas identified as having significant flood risk. According to the FD, a “flood” is defined as a temporary covering by water of land not normally covered by water. This encompasses floods from rivers, mountain streams, temporary watercourses, and sea flooding in coastal areas, but may exclude flooding caused by sewer systems. In comprehending the data, it is essential to differentiate between "hazard" and "risk". The definition of the risk concept presented in the "Operational Guidelines" of the Italian Ministry of the Environment, Land, and Sea (MATTM) follows the Varnes formula and defines risk as the product of three parameters: hazard (P), vulnerability (V), and exposure (E), expressed as R = P x V x E = P x Dp. Hazard (P) refers to the probability of a specific event occurring within a certain site over a defined return period. Vulnerability (V) is associated with the capacity of an element to withstand the event. Exposure (E) relates to the value of the exposed element in terms of human lives, economic assets, cultural heritage, and more. The Potential Damage (Dp) is the expected loss resulting from a natural event of a specific intensity, which depends on both the value and vulnerability of the exposed element (Ercoli, 2019). The present thesis focuses on the analyzing the Social Vulnerability Exposure (SVE), defined by the interplay between flood hazard and social vulnerability: SVE = P x V.

Regarding the Flood Hazard (P) ISPRA focuses on classifying flood-prone areas into high, medium, or low probability zones, based on their critical return time. In terms of the framework and investigated areas, the methodology spans three distinct domains: natural watercourses, artificial drainage networks in plains, and coastal areas (Lastoria et al., 2021). This multi-faceted approach ensures that the flood hazard mapping and risk assessment are comprehensive, considering the unique features and challenges of each domain. When mapping flood hazard in natural watercourses, hydrological and hydraulic models are employed. These models consider various factors such as precipitation, basin morphology, and topography to accurately estimate flood discharges and levels. For artificial drainage networks within plains, the approach involves historical data, hydrological models, and expert judgment to identify flood-prone areas. In coastal regions, geographic data analysis models are utilized to compute factors like sea surface elevation, including waves, tides, and surges. Based on this framework, the resulting flood hazard maps demarcate geographic areas that could be affected by floods under three hazard scenarios: high probability hazard (HPH), events with a return period between 20 and 50 years; medium probability hazard (MPH), events with a return period between 100 and 200 years; low probability hazard (LPH), events with a return period of up to 500 years (Lastoria et al., 2021). This classification provides a structured approach to understanding and managing flood risks and forms the basis for informed decision-making by urban planners, emergency responders, and policymakers.

The "Operational Guidelines of the Ministry of the Environment, Land and Sea" classify "Exposed elements" (E) encompassing population, strategic structures, key infrastructure, environmental, historical, and cultural assets, economic activities, and industrial or environmentally hazardous sites, including protected areas potentially affected by floods (Ercoli, 2019). In order to evaluate the potential damage (Dp), a vulnerability assessment is needed. Given the complexity of determining the resistance of diverse assets to extreme events, a simplifying assumption assigns a vulnerability value (V) of 1 to all elements within the six categories, facilitating the transition from exposed element maps to potential damage maps, where estimated damage equals the exposed element's value (Lastoria et al., 2021). The assumption of assigning a uniform vulnerability value of 1 to all elements is challenged in this study as it falls short in capturing crucial information regarding the strengths and weaknesses of a population in the face of natural disasters. The analysis of municipal level data enables to assess varying levels of vulnerability throughout the region and by intersecting this information with flood hazard data it offers new dimensionality to the analysis.

3.2. Study Area: Emilia-Romagna

Emilia-Romagna, a region rich in cultural heritage and economic productivity, is situated in the North of Italy and located at the base of the Apennine Mountains. The region's susceptibility to flooding is closely linked to its geological setting. The region witnesses the convergence of 14 rivers, contributing to the potential for riverbanks to overflow during intense rainfall events. The vast floodplain within Emilia-Romagna, the so-called Po Valley, carries this heightened risk of flooding when rivers exceed their capacity. The valley comprises alternating layers of clay, silt, and sand, with clay rocks being among the least permeable in nature. This impermeability impedes efficient water infiltration, causing water to accumulate on the surface, ultimately resulting in widespread flooding (Brandolini et al., 2015). Meteorological factors further compound the flood risk. The persistence of low-pressure areas over the region causes prolonged and intense rainfalls. Emilia-Romagna's mountainous terrain acts as a barrier affecting weather patterns, further influencing the protracted nature of these rainfall events (Fuchs et al., 2022). While a direct causal link between these floods and climate change remains scientifically uncertain, there exists a broader correlation between global temperature increases and the frequency of extreme weather events. Global warming may amplify the extremes of hot and cold, leading to more frequent occurrences of droughts and floods (Kotroni et al., 2016). The towns most affected by flooding are positioned along the boundary between the Apennines and the adjacent plains. These towns bear the brunt of heavy rainfall due to their geographical alignment, as the rainwater from the Apennines flows into a network of rivers that traverse the region, perpendicular to the mountain chain's direction. At the same time these town are urban centers, such as Bologna, Modena, and Parma, hubs of industry, education, and tourism. It is in fact the concentration of infrastructure and population in these areas that magnifies the potential impact of flooding. Urbanization has led to significant land-use changes, with "cementification" altering the natural landscape and significantly decreasing the capacity of the soil to absorb water (Schumm & Lichty, 1984).

This high flood hazard in Emilia-Romagna is reflected in the data provided by ISPRA. As discussed earlier, the ISPRA classification system delineates three levels of flooding probability to outline the extent of flood-prone areas across the entire national territory in accordance with Article 6 of the Floods Directive. Italy's geographic administration operates on multiple levels, encompassing 20 regions, which in turn comprise 107 provinces (province), and further splintered into approximately 7.900 municipalities (comuni). In this study, we focus on the municipality level, providing insights at a highly granular scale. *Table 1* depicts the percentage of regional territory affected by floodable areas for the three flood probability scenarios and values calculated at the national scale. *Figure 1* in the Appendix displays for each probability scenario the correlating

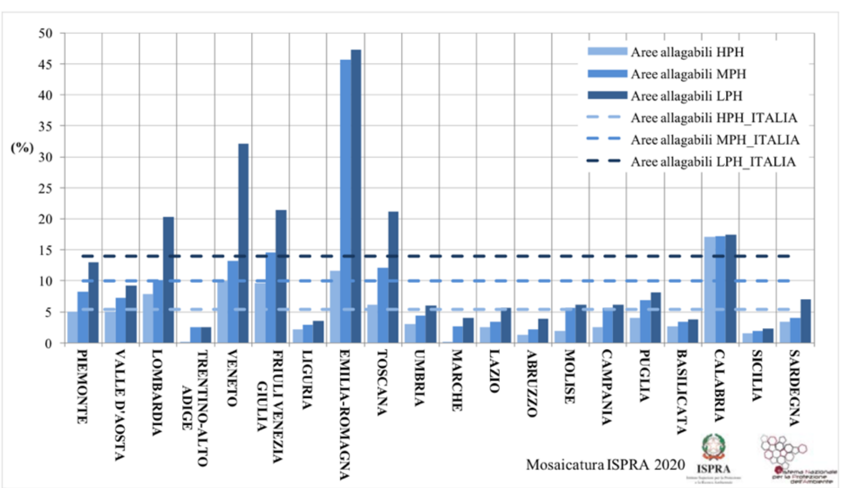

Table 1. *Percentage of regional territory affected by floodable areas for the three flood probability scenarios and values calculated at the national scale.*

spatial distribution of the potential flood-prone areas for Italy. These statistics show that Emilia Romagna is the region with the highest flood hazard probability. The floodable areas for all three flood probability scenarios exceed the national average. Specifically, Emilia Romagna has the highest percentage of floodable territory for both the low and medium probability scenarios across all of Italy.

3.3. Northern Apennines Hydrographic District

In Italy, hydrographic districts are organized according to river basins. Emilia-Romagna encompasses one major hydrographic district: the Northern Apennines District, which includes the Po River basin (*Figure 2* in Appendix). These districts are pivotal in managing water resources and addressing flood risks in the region. The territory under the jurisdiction of the Northern Apennines District affects eight Italian regions, with Emilia-Romagna covering an area of 22,406 km² (Lastoria et al., 2021). Given the Po basin's considerable size and the diversity of flood processes along its river network, hazard mapping adopts different methodological approaches for the various territorial areas. This distinction is unique to the Po basin's Unit of Management (UoM) and not applied to other UoMs within the district. Hydrological and hydraulic modeling is primarily used for the main river network and only locally for secondary networks and other territorial areas. In the latter cases, a morphological or historical-inventory approach is generally adopted (Lastoria et

Figure 3. *Floodable surface areas for the various UoMs of the Po River Hydrographic District under different probability scenario*

al., 2021). *Figure 3* maps the floodable surface areas for the various UoMs of the Po River Hydrographic District under different probability scenarios. While in Emilia-Romagna hazard scenarios in flood-prone areas are generally classified on the basis of above-mentioned return periods (20-50 years (HPH), 100-200 years (MPH), and up to 500 years (LPH)), shorter return periods are applied for marine coastal areas: 10 years (HPH), 100 years (MPH), and over 100 years (LPH), (Lastoria et al., 2021).

4. Methodology

4.1. Constructing and mapping of socio-economic indicators

For constructing the socio-economic indicators, the study draws upon a diverse set of demographic and social characteristics as well as housing details to outline the social structure of the population. To specifically address social vulnerability in Italy specifically, a set of five primary indicators is identified. The literature on social vulnerability in the context of natural hazards unveils a broad consensus about some of the most relevant factors that determine social vulnerability. Works like Cutter et al. (2003), Birkmann (2006), Utami (2008), or Cutter et al. (2009) frequently cite age, income levels, employment status, and education as important factors that influence how individuals and communities understand and respond to potential threats. In addition to these four aspects residential property is considered as fifth indicator for the analysis. In order to construct all these indicators five proxy variables are used to capture the socio-economic conditions influencing a community's capacity to prepare for, respond to, and recover from hazards and disasters. For implementation, data from the 15th Population and Housing census from 2011 was collected at the municipality level (ISTAT, 2012).

The *Age* indicator is expressed by the share of population that is 65 or older, reflecting the heightened vulnerability of the elderly, taking into account aspect such as dependence, mobility, literacy, and economic security (Blaikie et al., 2014). *Income* is proxied by taxable income and relates to the limited ability to prepare for and recover from such natural hazards. *Unemployment* is defined by the unemployment rate and relates to the vulnerability brought on by job loss, in particular due to limited financial resources, housing options, access to resources like insurance, or reduced capacity for recovery. Also, the raised risk of job loss after a disaster can lead to increased unemployment rates, particularly in low-paying jobs that are more prone to closure or relocation (Morrow, 1999). *Education* is proxied by the share of population with secondary education and adresses the understanding of emergency protocols. It is also linked to the socio-economic status, as it is connected to better job opportunities and higher income (Elstad, 1996). Lastly, *Residential Property* is proxied by the share of buildings constructed after 1960 and connects to modern construction standards that are less prone to damage during disasters. The setting of 1960 as a threshold year is based on post-war changes in urban development and flood risk management approaches in Italy. All these considerations highlight that social vulnerability is closely linked to social disparities, stemming from differences in income, social class, and education, as noted by Blaikie et al. (2014), and Bolin & Stanford (1991). The five indicators and their respective proxy variables as well as the direction of their impact on social vulnerability are depicted in *Table 2*.

For a comprehensive understanding of their spatial distribution, the socio-economic indicators developed for this study are transformed into geographical data using Geographic Information Systems (GIS) software, specifically QGIS. This transformation allows for the creation of maps

Table 2. *Variables, indicators, and their impact on social vulnerability*

Indicator	**Proxy Variable**	**Impact on social vulnerability**
Age	Share of population that is 65 or older (%)	Increase
Income	Taxable income (€)	Decrease
Unemployment	Unemployment rate (%)	Increase
Education	Share of population with secondary education (%)	Decrease
Residential Property	Buildings after constructed after 1960	Decrease

that provide a visual representation of the distribution of these indicators across the region. Given Emilia-Romagna's considerable diversity, this information is crucial in emphasizing the role of each factor in shaping the overall social vulnerability of a particular location. This study capitalizes on granular analysis to uncover critical variations and patterns that are often missed in macro-scale studies, thereby enhancing the precision and effectiveness of policy interventions.

4.2. Constructing and mapping of social vulnerability index

In order to assess overall social vulnerability, the socio-economic indicators must be combined into a single measure: the Social Vulnerability Index (SVI). Given the lack of a single approach in assigning weights in social vulnerability studies (Rygel et al., 2006), various authors have adopted different weighting methods. In this study, the socio-economic indicators are weighted according to the approach of Frigerio et al. (2016), using the Principal Component Analysis (PCA). This statistical method allows to analyze indicators, uncovering underlying relationships between variables and highlighting the most significant dimensions. Since the five indicators are measured in different ways, the first step requires data standardization, transforming the data to have a mean of 0 and a standard deviation of 1. Subsequently the PCA is applied. By this method five factors, each a linear combination of the five socio-economic indicators, their corresponding eigenvalues, and the proportion of variance each factor explains are computed (*Table 3-4* in Appendix). Only factors with an eigenvalue larger than one are considered for the construction of the SVI, hence *factor1* and *factor2*. These two factors together explain the relationship between all variables and account for a total of 74% of the variance in the dataset. For each municipality the factor scores are calculated and weighted according to Siagian et al. (2014), by multiplying them with their respective variance percentages and dividing by the total variance. As a result, we obtain the formula for calculating the SVI: $SVI = \frac{0{,}508*factor1}{0{,}74} + \frac{0{,}232*factor2}{0{,}74}$

Once the SVI for each municipality is computed, its spatial distribution is derived by mapping the data with QGIS. Such a representation enables a detailed assessment of social vulnerability which is crucial for effective decision-making and targeted interventions in vulnerable communities.

4.3. Correlation analysis between socio-economic indicators and flood hazard

The research methodology adopted in this study encompasses a multi-step approach for evaluating the socio-economic vulnerability in Emilia-Romagna concerning flood hazards. To achieve this aim, the next step involves conducting a correlation analysis between the flood hazard indicators and the socio-economic indicators. The flood hazard indicators correspond to the percentage of territory within each municipality that is prone to flooding under the three distinct flood probability scenarios, as provided by ISPRA: high probability hazard (HPH), medium probability hazard (MPH), low probability hazard (LPH). The availability of data at municipality level for both socio-economic indicators and flood hazard enables a comprehensive analysis of their interrelationship. The results obtained from the correlation analysis are visualized in heatmaps in Section 5, which serve to highlight correlation coefficients by employing a color-coded scheme, simplifying the interpretation of the strength and direction of these correlations.

It is important to acknowledge a limitation in interpreting the data used for this analysis: the socio-economic indicators are derived from the 15th Population and Housing Census of Italy, published in 2011, while the flood risk data is from 2020. This nine-year interval presents a noteworthy temporal discrepancy. The 2011 census data, despite being the most recent comprehensive dataset available, may not fully reflect the current socio-economic conditions in Emilia-Romagna, which could have evolved significantly over the years. Between 2011 and 2020, Emilia-Romagna likely experienced various changes, including economic fluctuations, demographic shifts, policy changes, migration trends and technological advancements. These factors, along with environmental and climatic changes, could have altered the socio-economic fabric of the region and its vulnerability to flooding. Nevertheless, the 2011 Census data provides valuable insights into the regional disparities and social structures that influence vulnerability to flooding. As an upcoming Population and Housing Census is expected to be published in 2024, this presents an opportunity for future research to apply the same methodology with updated data. Throughout the nine-year period, this study did take into consideration municipal mergers when conducting correlations and mapping geographical data, ensuring accuracy and relevance in its analysis.

4.4. Assessing and mapping social vulnerability exposure

One significant benefit of combining the SVI map with flood hazard maps is the development of social vulnerability exposure maps, as suggested by Frigerio et al. (2016). This integrated approach is instrumental in identifying areas where social factors might intensify the impacts of flood hazards. To examine the spatial interplay between flood hazard and social vulnerability, we employ the risk assessment matrix illustrated in *Figure 4*. For this analysis, both the SVI scores and the flood hazard indicators for each probability scenario are categorized into four distinct classes – 'Very Low,' 'Low,' 'Medium,' and 'High' – using the quantile classification method. Within each probability scenario, we then merge the flood hazard and SVI classes following the matrix. This enables us to categorize the Social Vulnerability Exposure (SVE) of each municipality into four corresponding groups. The resultant data forms the basis for creating detailed SVE maps. The maps reveal hotspot areas characterized by a combination of high flood hazard and increased social vulnerability.

Figure 4. *Risk assessment Matrix*

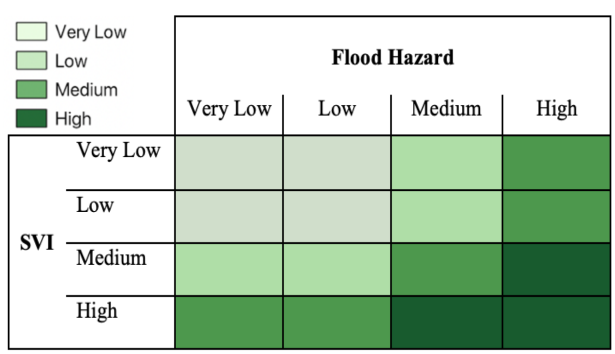

5. Results and discussion

As outlined in Section 4.2, the Social Vulnerability Index is constructed utilizing PCA and mapped with QGIS. *Figure 5* displays the spatial distribution of SVI across Emilia-Romagna, showing significant variations within the region, represented by Boxes A to C. To improve the interpretability of these findings, Corine Land Cover (CLC) data is used to provide insights into the diverse land cover patterns within the Emilia-Romagna region (*Figure 6*). The combination of these two maps reveals that Box A consists of municipalities with large urban centers, such as Bologna, Modena, and Parma, the three biggest cities in the region. Box B comprises municipalities that are primarily rural, located at significantly higher altitudes in the Apennine Mountains and immersed in forest and semi-natural areas. The municipalities in Box C extend along the coast and are mainly covered by agricultural areas, wetlands and some urban centers. A granular analysis of each socio-economic indicator is important for interpreting the results in order to understand what role the individual factors play in the allocation of the SVI. *Figure 7* presents the spatial distribution of the five socio-economic indicators across Emilia-Romagna, constructed and mapped as outlined in Section 4.1.

Figure 5. *Social Vulnerability Index map for Emilia-Romagna*

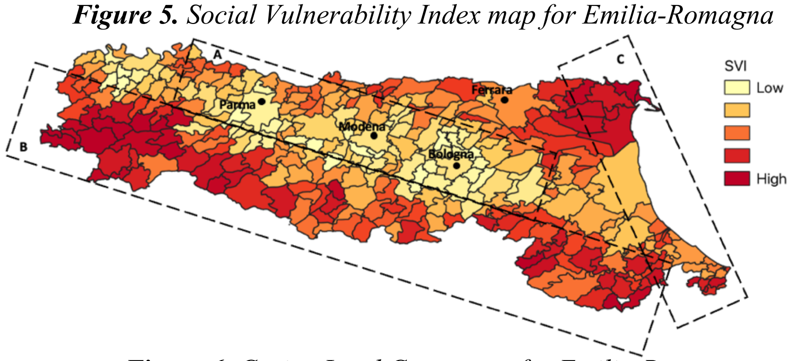

Figure 6. *Corine Land Cover map for Emilia-Romagna*

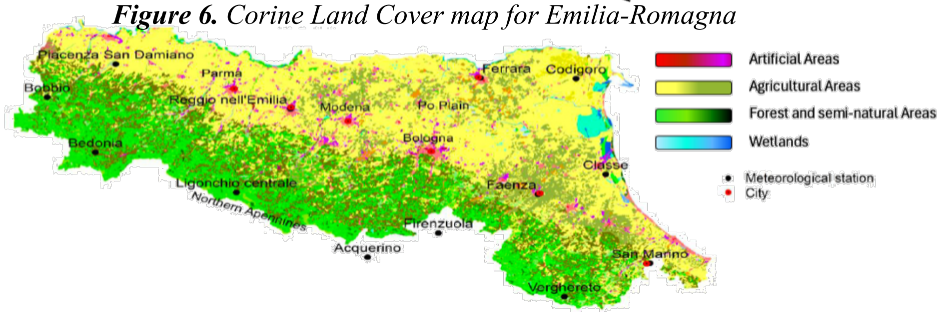

The lighter shaded areas in Box A indicate a low SVI and mainly comprise municipalities with urban centers. They are marked by high levels of income that reflect the variety of the economic activities in the region. This area in Emilia-Romagna is home to major automotive companies like Ferrari and Lamborghini and hence claims a strong industrial sector. The industrial strength, combined with thriving service and commercial activities, sets these municipalities apart from the predominantly agricultural rural ones. Similarly, employment patterns for municipalities in Box A reflect the economic dynamism of the region and reveal lower unemployment rates, compared to rural and mountainous regions. This is attributed to the concentration of industries and commercial activities in this area, creating a robust economic environment with diverse job opportunities. The map also illustrates higher levels of educational attainment in this area, due to the concentration of educational institutions and the continuous urban fabric that facilitates access to such facilities. Also, education in the urban centers aligns with the region's reputation for academic excellence, as institutions like the University of Bologna, one of the oldest universities in the world, are located here. The demographic distribution tends to be younger, likely influenced by the migration of the

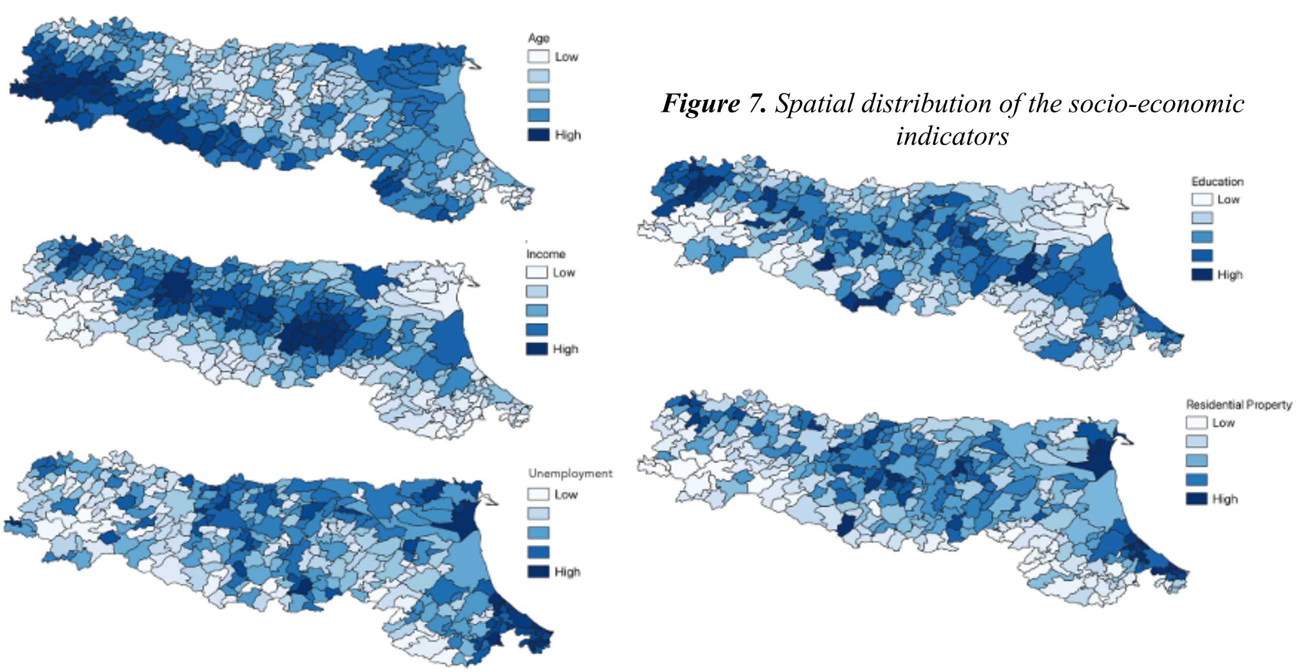

Figure 7. *Spatial distribution of the socio-economic indicators*

younger workforce towards urban centers for education and employment opportunities. This is particularly evident in Bologna, where a large student population contributes to a lively and youthful population. Lastly, the presence of newer residential buildings, as indicated by the residential property map, suggests a trend of more recent development for the municipalities comprised in Box A and reflects investment and infrastructural resilience (Brandolini et al., 2015). All these findings align with the expectation that urban centers are typically less vulnerable and explain why the SVI map shows lighter colors for this area. One interesting deviation from this pattern is represented by Ferrara. Even being an urban center, Ferrara lies in an area with higher vulnerability compared to the other cities. Ferrara is considered one of the “oldest” cities in Italy, with a significant aging and declining population. The depopulation trend, especially among the younger demographic, may lead to a lower score in education indicators, as there are fewer individuals to engage with educational institutions. These factors contribute to a higher SVI for Ferrara.

The municipalities in Box B are marked by darker shades indicating a high SVI and lie predominantly in mountainous regions. In these areas, the income levels are significantly lower, which is largely due to the heavy reliance on agriculture and the lack of jobs in industry or the service sector, which generally offer higher wages. These economic challenges and job market constraints are also reflected in the higher rates of unemployment. Educational attainment in these mountainous regions is lower than in urban areas. The limited number of educational institutions and challenging accessibility due to the geographical condition make it more difficult for residents to pursue education. The demographic composition is characterized by an aging population, as younger people relocate to urban areas in search of better education and employment opportunities. Additionally, the pace of development in these mountainous areas is slower than in urban regions. This is evident in the prevalence of older buildings, which is likely a result of the difficult topography and limited economic growth that have led to a slower rate of modernization and infrastructure development compared to the more rapidly developing urban areas (Fuchs et al., 2022).

Lastly, Box C encompasses municipalities with medium to high SVI that extend along the coast. Here the interplay of socio-economic indicators as a result of the reliance on tourism, which is seasonal in nature, results in a higher SVI. The influence of seasonal tourism leads to variable employment and income levels, with higher unemployment rates during off-seasons. Lower educational attainment in such areas is especially pronounced when the local workforce is primarily engaged in seasonal service occupations rather than in year-round employments that require higher education. The demographic composition reflects this combination of an aging permanent population and a younger, seasonal workforce.

In synthesis, it can be concluded that the granular analysis of each socio-economic indicator allows for a detailed understanding of the spatial distribution of the SVI across the region. The SVI map combines the effect of all five factors into one and provides decision makers with a valuable visualization for emergency management and territorial planning (Frigerio et al., 2016).

As described in Section 4.4 the social vulnerability exposure (SVE) serves to locate hotspot areas characterized by both high flood hazard and high SVI. In order to enhance this qualitative analysis first a quantitative evaluation of the correlation between flood hazard and socio-economic

Table 5. *Correlation Coefficients with p-values*

	education	residential property	unemployment	age	income
HPH	0.11 (p≈0.052)	0.23 (p≈0.000)	0.10 (p≈0.060)	-0.21 (p≈0.000)	0.15 (p≈0.005)
MPH	0.11 (p≈0.040)	0.35 (p≈0.000)	0.14 (p≈0.015)	-0.35 (p≈0.000)	0.25 (p≈0.000)
LPH	0.13 (p≈0.022)	0.37 (p≈0.000)	0.15 (p≈0.007)	-0.38 (p≈0.000)	0.28 (p≈0.000)

indicators is conducted, as explained in Section 4.3. *Table 5* provides the correlation coefficients along with their corresponding p-values. These results illustrate that each socio-economic indicator maintains the same directionality across the three flood hazard scenarios. Furthermore, the strength of the correlation for education and unemployment indicators remains quite consistent, irrespective of the flood hazard level. In contrast, residential property, age, and income indicators show a strengthening correlation as the probability of flood risk decreases. In order to interpret these results, it is necessary to take into consideration the distribution of flood hazard across the region. *Figure 8* displays for each municipality the percentage of its area at different flood probability scenarios, high (HPH), medium (MPH) and low (LPH). The darker shares in maps clearly illustrate that, in all three scenarios, flood-prone areas are primarily concentrated in the Po floodplain and coastal regions. According to the CLC data, these areas are characterized by multiple urban centers and industrial hubs. Conversely, the lighter shaded areas are mainly found in the Apennine mountainous, characterized by more rural and natural surfaces. The geographical distribution of flood hazards provides a contextual backdrop for interpreting these results. The negative correlation between the share of elderly population and flood hazard probabilities suggests a demographic trend where older individuals are more likely to reside in rural areas, often situated in the less flood-prone Apennine mountains. This pattern could be influenced by a variety of factors, including the pursuit of quieter, more stable living conditions, the continuation of historical settlement patterns but also the depopulation of rural areas especially by the younger generations.

Figure 8. *Percentage of area of a municipality at different probability hazard levels*

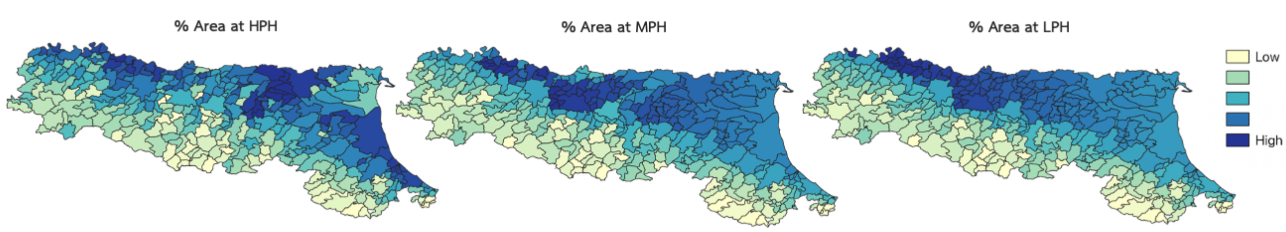

Income levels show a positive relationship with flood risk. Interestingly, this positive correlation grows stronger as the flood hazard decreases. Given that larger cities in Emilia-Romagna tend to be situated in low-hazard areas and these urban centers traditionally harbor higher-income populations, the increasing correlation coefficient in areas of lower flood probability is consistent with the socio-economic profile of larger urban areas. There is a positive correlation of unemployment with flood hazard areas. This relationship suggests that areas with higher flood risks, while offering more job opportunities, may also have higher population density and more competitive job market, leading to higher unemployment rates. Additionally, frequent flooding can disrupt local economies and businesses, potentially leading to job losses and economic instability, which could lead to an increase in unemployment. The correlation between education and flood hazards is relatively weak across all probabilities, possibly because the share of residents with a high school diploma does not significantly determine their place of residence in relation to flood risk areas. The presence of urban centers and industrial hubs does explain the positive sign of the correlation, however, it's worth noting that in Italy educational access and investment in educational infrastructure provide educational opportunities across the whole region. The correlation between residential property age and flood risk is significant, with newer buildings often located in flood-prone areas. This trend might reflect a prioritization of urban expansion over environmental risk considerations. It is important to note that newer constructions are likely to adhere to more stringent building codes and utilize advanced construction technologies designed to withstand environmental stresses, including floods. Therefore, despite being situated in flood-prone areas, these buildings may be less vulnerable to damage thanks to enhanced design standards and resilience measures.

The results obtained from this correlation analysis provide valuable insights to the interplay between each socio-economic component and the flood hazard and create the base for understanding the spatial distribution of the SVE in Emilia-Romagna. When overlaying the flood hazard data with the SVI, as depicted in the SVE map (*Figure 9*), a new dimension emerges. The figure shows that for all three flood hazard probability scenarios the spatial distribution of SVE is not significantly different. In examining the flood hazard levels, it's apparent that the Po plain are areas of high flood probability. However, as the SVI in these areas is low compared to other parts of the region, the SVE map reveals that most municipalities show a very low to medium SVE. This suggests that although these areas are more prone to flooding, stronger socio-economic structures can help buffer against the impact of floods. Therefore, while urban areas may have higher flood hazard due to their dense infrastructure and impermeable surfaces, their populations often benefit from stronger socio-economic structures. Factors such as higher average incomes, younger population and better education systems contribute to mitigating the impacts of floods. Populations in these areas generally have greater access to information and resources, which facilitates quicker recovery and more effective emergency responses. Additionally, urban planning often includes investments in infrastructure resilience, such as flood defenses and water management systems, that reduce the vulnerability of these populations to flood hazards. For example, the 2014 flood in Modena showcased the resilience of urban systems, where the impact on the population was mitigated

Figure 9. *Social Vulnerability Exposure map*

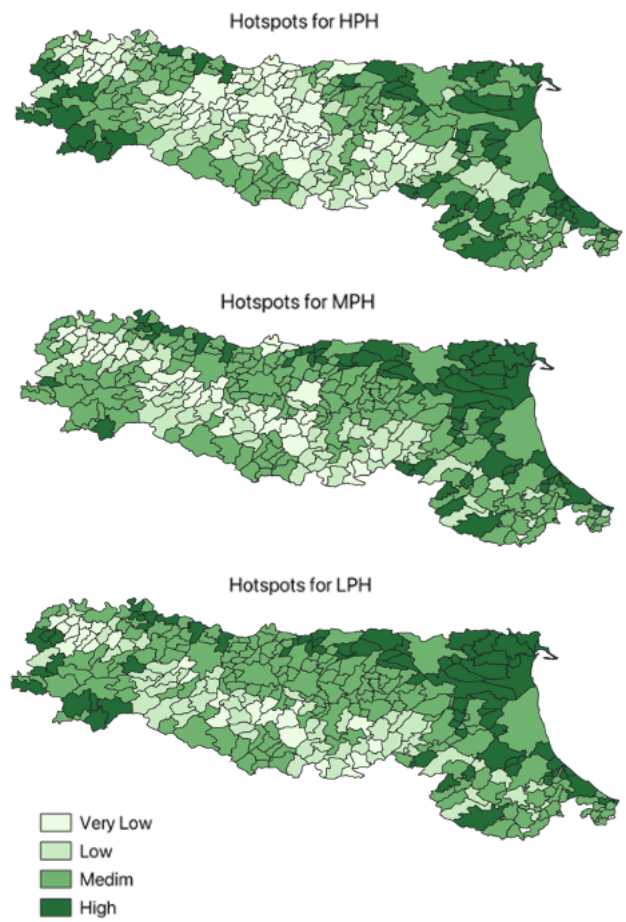

through effective emergency protocols and infrastructure. Policy makers must balance urban development with flood risk management, emphasizing sustainable urban planning that includes green spaces and improved drainage systems, and fostering community engagement and education on flood risks and preparedness. Contrastingly to this area, in the Apennine Mountain part some municipalities show medium to high SVE. This result stems from the fact that even though these areas have a very low probability of flooding, they show a high SVI, indicating weaker socio-economic structures. In this area, strengthening infrastructure, particularly transportation and sustainable housing, would improve connectivity and living conditions. Community engagement programs on emergency preparedness and sustainable practices could empower residents and foster resilience against natural and socio-economic challenges. The National Council of Geologists proposed the so called "Territorial Garrison", suggesting a shift towards more proactive and localized risk management (Panza et al., 2013). This concept of constant monitoring of vulnerable areas by geologists and engineers could be pivotal in early risk identification, communication and mitigation. Lastly, the coastal zones, depict the highest levels of SVE. These municipalities not only have areas with high probability of flooding but also exhibit medium to high social vulnerability. The municipalities in these areas represent the hotspots where flood hazard and SVI are both high. Here the focus should be on increased public awareness and political responsiveness towards flood hazard. The recognition of the need to integrate social vulnerabilities into flood risk management is exemplified by the approach taken in a study by Ciavola et al. (2018) conducted on the Emilia-Romagna coast, where local-scale post-event assessments were carried out using GPS and UAV-based quick-response surveys. This pilot case, following an extreme meteorological event in February 2015, demonstrated the effectiveness of integrating high-resolution physical data collection with qualitative information from local stakeholders. By capturing both the physical impact and the social dimension of the event, this methodology provided a more comprehensive understanding of the flood's effects. (Ciavola et al., 2018).

Although being based on a qualitative analysis, this last step of mapping the SVE serves as a preliminary stage in recognizing the spatial distribution of social vulnerability and identifying municipalities that display higher SVE and therefore need a more detailed examination (Frigerio et al., 2016). This analysis highlights that favorable socioeconomic conditions can mitigate flood hazard. The map can be a powerful tool for disaster impact modeling or developing risk mitigation strategies like those in the National Plan for Flood Risk Prevention. Incorporating human vulnerability analysis ensures that the interactions between societal structures and flood hazards are fully understood. It allows to identify and support vulnerable populations who may find it challenging to respond to and recover from flood events. Italy's established civil protection system, reformed by the 2018 Civil Protection Code, exemplifies a comprehensive approach towards disaster risk management (Alexander, 2018). This system involves various levels of government in activities aimed at protecting lives, properties, and the environment. In line with this approach, a participatory system dynamics modeling method was employed in the Bradano River case study in Italy, which facilitated collaborative flood risk management by overcoming technical and institutional barriers often faced by flood management agencies. This methodology exemplifies the importance of stakeholder engagement in developing effective flood risk management strategies (Giordano et al., 2020). The implementation of the EU Floods Directive (2007/60/EC) further reinforces this approach by providing a framework for assessing and managing flood risks across Europe. The response to the 2023 floods in Emilia-Romagna highlighted both the strengths and areas for improvement in Italy's disaster management strategies. The Italian government's approval of a 2 billion euros emergency relief package addressed the immediate aftermath of the floods. The region's ability to adapt quickly, including closing schools and urging remote work to facilitate emergency responses, demonstrated a notable level of preparedness and adaptability. However, the magnitude of the disaster also underscored the need for more robust long-term strategies, by improving not only the physical infrastructure but also strengthening social support systems, particularly in vulnerable communities. This involves a proactive approach to investing in preventive measures and enhancing community resilience against future hydrological events.

6. Conclusion

This study offers a comprehensive framework that integrates socio-economic analysis with flood hazard assessment in Emilia-Romagna. The distinctive approach of separating the methodology and result into multiple sections — socio-economic indicators, flood hazard, social vulnerability (SVI), and social exposure (SVE) — provides a detailed analysis of the region's susceptibility to flooding. This approach is strengthened by the use of municipality-level data and Geographic Information Systems (GIS). By combining SVI with flood hazard maps this study creates a qualitative social vulnerability exposure (SVE) map. Particularly notable in the SVE results is the diverse interplay between SVI and flood hazard areas across the region, with a significant convergence observed in coastal areas, thereby pinpointing areas that necessitate more detailed analysis. The key contribution of the spatial mapping of each metric across Emilia-Romagna is the visualization of the geographical variations and the creation of informative maps that are valuable for policymakers and for conveying complex information to a broader audience. One of the central takeaways from this analysis is the understanding that social vulnerability can either mitigate or exacerbate the resilience to flood hazards and it is therefore crucial to implement a more holistic approach to disaster management that considers both the physical risks and the underlying social fabric of the regions. It is crucial for future research and policy development to continue exploring these dynamic relationships to enhance regional resilience and preparedness.

7. Bibliography

Adger, W. N. 2010. “Social capital, collective action, and adaptation to climate change.” *Der klimawandel*: 327-345.

Alexander, D.E. 1993. “Natural Disasters.” London and New York: UCL Press and Chapman & Hall.

Alexander, D. 2018. “Civil protection in Italy-coping with multiple disasters.” *Contemporary Italian Politics* 10 (4): 393-406.

Arrighi, C., and A. Domeneghetti. 2023. “Brief communication: On the environmental impacts of 2023 flood in Emilia-Romagna (Italy).” *Natural Hazards and Earth System Sciences Discussions* 2023: 1-10.

Birkmann, J. 2006. “Indicators and criteria for measuring vulnerability: Theoretical bases and requirements.” In *Measuring Vulnerability to Natural Hazards: Towards Disaster Resilient Societies*, 55–77.

Blaikie, P., T. Cannon, I. Davis, and B. Wisner. 2014. “At risk: Natural hazards, people's vulnerability and disasters.”

Bolin, R., and L. Stanford. 1991. “Shelter, housing and recovery: A comparison of U.S. disasters.” *Disasters* 15 (1): 24–34.

Brandolini, P., A. Cevasco, D. Capolongo, M. Galli, and M. Firpo. 2015. “Geohydrological hazards and urban development in the Mediterranean area: an example from Genoa (Liguria, Italy).” *Natural Hazards and Earth System Sciences* 15 (12): 2631-2646.

Chen, W., X. Wang, S. Deng, C. Liu, H. Xie, and Y. Zhu. 2019. “Integrated urban flood vulnerability assessment using local spatial dependence-based probabilistic approach.” *Journal of Hydrology* 575: 454-469.

Ciavola, P., Ó. Ferreira, P. Haerens, M. Van Koningsveld, C. Armaroli, and Q. Lequeux. 2018. “Local-scale post-event assessments with GPS and UAV-based quick-response surveys: a pilot case from the Emilia–Romagna (Italy) coast.” *Natural Hazards and Earth System Sciences* 18 (11): 2969-2989.

Cutter, S. L. 1996. “Vulnerability to environmental hazards.” *Progress in Human Geography* 20: 529–539.

Cutter, S. L., B. J. Boruff, and W. L. Shirley. 2003. “Social vulnerability to environmental hazards.” *Social Science Quarterly* 84 (2): 242-261.

Cutter, S. L., C. T. Emrich, J. J. Webb, and D. Morath. 2009. “Final Report to Oxfam America. Social vulnerability to climate variability hazards: A review of the literature.”

European Parliament and the Council. 2007. “Directive 2007/60/EC of the European Parliament and of the Council of 23 October 2007 on the assessment and management of flood risks.” *Official Journal of European Communities*, L 288: 27–34.

Elstad, J. I. 1996. “Inequalities in health related to women’s marital, parental, and employment status a comparison between the early 70s and the late 80s, Norway.” *Social Science & Medicine* 42 (1): 75–89.

Ercoli, P. 2019. “Mappe della pericolosità e del rischio [Maps of Hazard and Risk].” Regione Emilia-Romagna, Servizio Difesa del Suolo della Costa e Bonifica.

Frigerio, I., S. Ventura, D. Strigaro, M. Mattavelli, M. De Amicis, S. Mugnano, and M. Boffi. 2016. “A GIS-based approach to identify the spatial variability of social vulnerability to seismic hazard in Italy.” *Applied Geography* 74: 12-22.

Fuchs, S., M. Keiler, S. Sokratov, and A. Shnyparkov. 2022. “Focus Issue: Addressing Challenges of Hazards, Risks, and Disaster Management in Mountain Regions.” *Mountain Research and Development* 42.

Giordano, R., I. Pluchinotta, A. Pagano, P. Pengal, and S. Santopietro. 2020. “A participatory system dynamics modeling approach to facilitate collaborative flood risk management: A case study in the Bradano River (Italy).” *Journal of Hydrology* 590: 124354.

Hoque, M. A. A., S. Tasfia, N. Ahmed, and B. Pradhan. 2019. “Assessing spatial flood vulnerability at Kalapara Upazila in Bangladesh using an analytic hierarchy process.” *Sensors* 19 (6): 1302.

ISTAT. 2012. “15° Censimento generale della popolazione e delle abitazioni. Struttura demografica della popolazione - Dati definitivi.”

Khajehei, S., A. Ahmadalipour, W. Shao, and H. Moradkhani. 2020. “A place-based assessment of flash flood hazard and vulnerability in the contiguous United States.” *Scientific Reports* 10 (1): 448.

Kotroni, V., K. Lagouvardos, and R. Deidda. 2016. “Preface: Advances in meteorological hazards and extreme events.” *Natural Hazards and Earth System Sciences* 16 (5): 1259-1261.

Lastoria, B., M. Bussettini, S. Mariani, F. Piva, and G. Braca. 2021. “Rapporto sulle condizioni di pericolosità da alluvione in Italia e indicatori di rischio associati.” Istituto Superiore per la Protezione e la Ricerca Ambientale (ISPRA).

Legge 49/2010. “Attuazione della Direttiva comunitaria 2007/60/CE relativa alla valutazione e alla gestione dei rischi di alluvioni.” Del 23 febbraio 2010.

Morrow, B. H. 1999. “Identifying and mapping community vulnerability.” *Disasters* 23 (1): 1–18.

Nistor, M. M., and G. C. G. Porumb. 2015. “How to compute the land cover evapotranspiration at regional scale? A spatial approach of Emilia-Romagna region.” *GEOREVIEW: Scientific Annals of Stefan cel Mare University of Suceava. Geography Series* 25 (1): 38-53.

Pachauri, R. K., M. Allen, V. Barros, J. Broome, W. Cramer, R. Christ, et al. 2007. “Climate change 2007: Synthesis report. Contribution of Working Groups I, II and III to the Fifth Assessment Report of the Intergovernmental Panel on Climate Change.”

Panza, G., S. Sparnocchia, T. Georgiadis, A. Mugnai, and I. I. Altieri. “Italian Report on IAMAS-IUGG activities 2012-2013.”

Remo, J. W., N. Pinter, and M. Mahgoub. 2016. “Assessing Illinois’s flood vulnerability using Hazus-MH.” *Natural Hazards* 81: 265-287.

Rufat, S., E. Tate, C. G. Burton, and A. S. Maroof. 2015. “Social vulnerability to floods: Review of case studies and implications for measurement.” *International journal of disaster risk reduction* 14: 470-486.

Rygel, L., D. O’sullivan, and B. Yarnal. 2006. “A method for constructing a social vulnerability index: An application to hurricane storm surges in a developed country.” *Mitigation and Adaptation Strategies for Global Change* 11 (3): 741–764.

Schumm, S. A., and R. W. Lichty. 1984. *Developments and applications of geomorphology.* Springer-Verlag.

Siagian, T. H., P. Purhadi, S. Suhartono, and H. Ritonga. 2014. “Social vulnerability to natural hazards in Indonesia: Driving factors and policy implications.” *Natural hazards* 70 (2): 1603–1617.

Thakuy, J.K., K.S. Singh, A. Ramanathan, and W. Gossel. 2011. *Geospatial Techniques for Managing Environmental Resources*, 308.

Trigila, A., C. Iadanza, B. Lastoria, M. Bussettini, and A. Barbano. 2021. “Dissesto idrogeologico in Italia: pericolosità e indicatori di rischio.” Istituto Superiore per la Protezione e la Ricerca Ambientale (ISPRA).

Uitto, J. I. 1998. “The geography of disaster vulnerability in megacities: A theoretical framework.” *Applied Geography* 18: 7-16.

Utami, P. 2008. “Measuring social vulnerability in volcanic hazards: The case study of Merapi volcano, Indonesia.” Ph.D. thesis, University of Bristol.

Welle, T., J. Birkmann, J. Rhyner, M. Witting, and J. Wolfertz. 2012. “Worldriskindex 2012: Concept, updating and results.” In *World Risk Report 2012*, 11–26.

Zheng, N., K. Takara, Y. Tachikawa, and O. Kozan. 2008. “Analysis of vulnerability to flood hazard based on land use and population distribution in the Huaihe River basin, China.”

Zhou, Q., P. S. Mikkelsen, K. Halsnæs, and K. Arnbjerg-Nielsen. 2012. “Framework for economic pluvial flood risk assessment considering climate change effects and adaptation benefits.” *Journal of Hydrology* 414: 539-549.

8. List of Figures and Tables

9. Appendix

Figure 1. The spatial representation of the potential flood-prone areas for Italy for each probability scenario

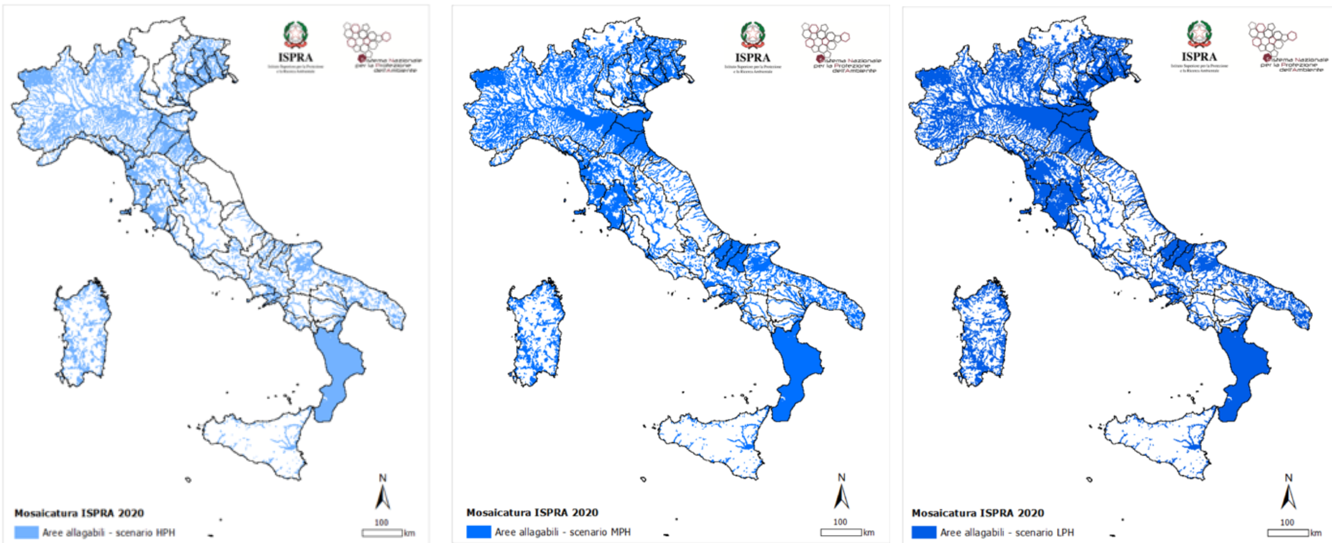

Figure 2. Breakdown of the territory of the Po River hydrographic district

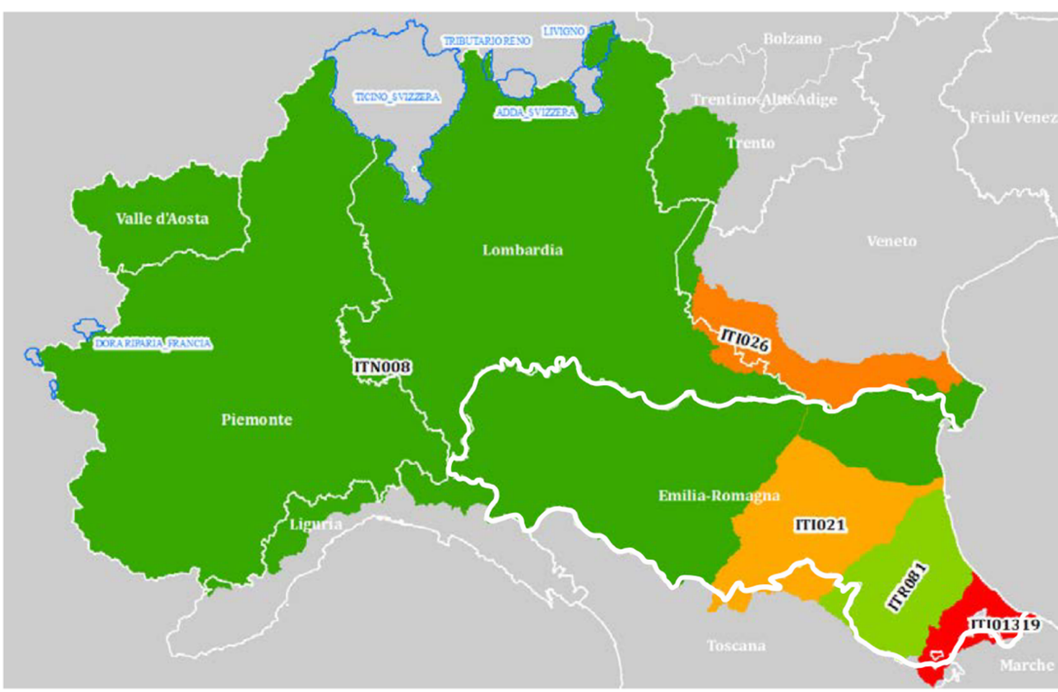

Table 3. *Results from PCA: factors, eigenvalues and variance explained*

Factor	Eigenvalue	Variance Explained
1	2.547 (>1)	50.8%
2	1.161 (>1)	23.2%
3	0.570	11.4%
4	0.408	8.1%
5	0.329	6.6%

Table 4. *Results from PCA: factor loadings*

Indicator	Factor 1	Factor 2	Factor 3	Factor 4	Factor 5
Education	-0.497	-0.252	-0.517	-0.344	0.551
Residential Property	-0.474	0.299	0.634	0.260	0.466
Employment	-0.015	0.859	-0.489	0.150	0.015
Age	0.524	-0.198	-0.172	0.571	0.575
Income	-0.504	-0.264	-0.250	0.683	-0.384